2.B:
2.E

Nuclear Physics **50** (1964) 479—488; © *North-Holland Publishing Co., Amsterdam*

OPTICAL MODEL AND DISTORTED WAVE ANALYSES OF (d, d), (d, p) AND (d, d') REACTIONS ON O^{16}, Ni^{58}, Pb^{207} AND Pb^{208} AT 27.5 MeV

J. TESTONI and S. MAYO

Comisión Nacional de Energía Atómica, Buenos Aires, Argentina †

and

P. E. HODGSON

Nuclear Physics Laboratory, Oxford

Received 18 June 1963

Abstract: Angular distributions for the elastic scattering of 27.5 MeV deuterons by isotopically-separated Pb^{207} and Pb^{208} targets together with the distributions of the proton groups resulting from stripping reactions to the ground states of Pb^{208} and Pb^{209} were measured using simple scintillation techniques with an energy resolution of 2.5 to 3 %. The elastic scattering data, together with similar data previously measured on O^{16} and Ni^{58}, were analysed using the diffuse-surface nuclear optical model with a volume absorption potential. The elastic scattering data were reasonably well fitted with model parameters obtained by an automatic least-squares procedure. Using the optical model parameters obtained from the elastic scattering analyses, the inelastic scattering and (d, p) stripping angular distributions were fitted by strong coupling and distorted wave Born approximation calculations.

1. Introduction

Although there are many nuclear optical model analyses of nucleon interactions at low and intermediate energies on a variety of nuclei, the corresponding analyses of deuteron interactions have only recently been made [1]). The present work extends elastic scattering analyses to a deuteron energy of 27.5 MeV and includes strong coupling and distorted wave computations of inelastic and deuteron stripping cross-sections with the optical model parameters obtained from the elastic scattering analyses.

Examination of the shapes of the experimental angular distributions of the particles from 27.5 MeV deuteron-induced reactions shows that distortion effects must certainly be considered when analysing such data. This is supported by the cases presented here, as the angular distributions for inelastic and stripping reactions cannot be explained in terms of plane wave theories.

Targets for the present experiments were chosen widely-spaced in the periodic table, and because of the poor energy resolution doubly or singly magic nuclei were preferred because of the energy gap to the first excited state, which makes possible the clear separation of the inelastic secondary particles.

† Work performed under the auspices of Consejo Nacional de Investigaciones Científicas y Técnicas, Argentina.

2. Experimental Procedure

The experimental arrangement and procedure used in the present work is the same as described previously [2]).

Lead targets were isotopically enriched and converted to foils of about 10 mg/cm^2 at the Oak Ridge National Laboratory. Their composition is as follows (in percent components): Pb^{207} target: 0.20 Pb^{204}, 7.02 Pb^{205}, 82.57 Pb^{207}, 10.21 Pb^{208}; Pb^{208} target: 0.05 Pb^{204}, 0.20 Pb^{206}, 0.05 Pb^{207}, 99.75 Pb^{208}.

The reaction products were detected at scattering angles every 5 degrees in the forward right quadrant and every 10 degrees in the backward left quadrant using a NaI(Tl) cylindrical crystal 1 cm in diameter and 0.5 cm thick mounted on a Philips 53AVP photomultiplier tube. The pulse-height analysis was performed with a single-channel analyser.

Spectra were obtained by using window widths of 1 V and checking the area under a peak with wider window widths up to 10 V. Statistical errors were kept below 10% in every case; however, the main source of error in evaluating peak areas arises from the background subtraction, especially for the inelastic groups.

The angular distribution for Ni^{58} was re-measured using the same experimental arrangement as above except that the spectra was displayed on a 128-channel Nuclear Data Model 120 analyser. No significant difference from the earlier measurements was found, except that the statistical errors were reduced.

The errors indicated on the figures by vertical bars include those arising from statistics, background subtraction, beam integration, target thickness, solid angle of detection and stability of the electronic equipment. The reproducibility of measurements was better than $\pm 5\%$.

The zero scattering angle was checked by measuring cross sections on both sides of the scattering chamber. The angular aperture of the detector was ± 0.5 degrees. The energy resolution was 2.5 to 3% and the linearity of the detecting system was checked with different particle groups from various known reactions.

3. Elastic Scattering Optical Model Analysis

The potentials used for the present analyses were of the simple form

$$V(r) = V_C(r) - (U + iW)f(r),$$

where r is the separation of the reacting nuclei; U and W are the refractive and absorptive strengths of the central spin-independent potential; $f(r) = \{1 + \exp[(r-R)/a]\}^{-1}$ is the Saxon-Woods form factor; $V_C(r)$ is the Coulomb potential due to a uniformly charged sphere of radius $R_C = 1.3A^{\frac{1}{3}}$ fm; $R = r_0 A^{\frac{1}{3}}$ and a are the nuclear radius and the surface diffuseness parameter, respectively.

No surface optical model potentials were considered in view of the rather high bombarding energies used. The computations were carried out on a Ferranti-Mercury

computer; the programme used included a least-squares automatic fitting procedure leading to a minimal Δ value for the optimum fit [3]). In each calculation the experimental data were normalized by multiplying by the optimum factor N. It was found that the calculations for O^{16} and Ni^{58} agreed with the experimental data when appropriate normalization was used. In order to confirm the correctness of the normalization the Ni^{58} elastic angular distribution was remeasured, as mentioned in sect. 2. Then a new fit to the data was made allowing the computer to find the best parameter set without using a normalization factor during the automatic fit. This calculation gave N-values close to unity together with Δ-values similar to those obtained when normalization was used during the searching procedure.

TABLE 1

Best fit optical model parameters for the elastic scattering of deuterons

Target	E_d (MeV)	U (MeV)	W (MeV)	r_0 (fm)	a (fm)	σ_R (mb)	Δ	N	l_{max}	Included exp. points	Normalization during search
O^{16}	26.3	53.1	9.9	1.63	0.38	870	530	0.59	13	all	yes
		56.9	12.0	1.50[a])	0.65[a])	990	1430	0.94	15	all	yes
Ni^{58}	27.5	49.9	12.7	1.59	0.48	1627	780	1.29	18	up to 100°	yes
		55.0	17.0	1.54	0.46	1540	1720	1.53	17	all	yes
		54.1	14.3	1.50[a])	0.65[a])	1720	2230	1.04	20	up to 100°	yes
		53.2	13.8	1.53	0.52	1581	262	1.15	18	up to 80°	no
		56.1	16.9	1.48	0.53	1520	730	1.13	18	all	no
Pb^{207}	27.5	60.6	18.3	1.47	0.55	2340	100	0.87	21	all	yes
Pb^{208}		53.8	9.3	1.50[a])	0.65[a])	2590	380	≈1.00	20	all	yes

σ_R is the total reaction cross-section.

The normalization factor $N = \Sigma_i(\sigma^i_{th}/\delta_i)^2/\Sigma_i(\sigma^i_{th}\sigma^i_{exp}/\delta_i^2)$.

$\Delta = \Sigma_i\{[(d\sigma^i/d\Omega)_{exp} - (d\sigma^i/d\Omega)_{th}]/\delta_i(d\sigma^i/d\Omega)_{exp}\}^2$.

$\delta_i(d\sigma^i/d\Omega)_{exp}$ is the error of the measured cross-section.

[a]) Fixed during search.

In a first set of runs the parameters U, W, a and r_0 were varied simultaneously; in a second set of runs the geometrical parameters a and r_0 were kept fixed at reasonable values ($a = 0.65$ fm and $r_0 = 1.5$ fm) while the potentials U and W were adjusted to give the best fit to the data; the agreement for the latter is not as good as that obtained by adjusting all the parameters. Table 1 shows the parameter values resulting from the present analyses. Table 2 shows the evolution of the calculated parameters as the computer was running. In both tables there are two sets of best fits; one set corresponding to a simultaneous variation of four parameters and the other set corresponding to two of them fixed as mentioned above.

In general the results show the same behaviour as those obtained for deuteron elastic scattering at lower bombarding energies.

These data have also been fitted by Satchler [4]) using a similar potential but allowing different from factors for the real and imaginary parts.

TABLE 2

Evolution of parameters for the elastic scattering of deuterons in the automatic fit

Target	Cycle	U (MeV)	W (MeV)	r_0 (fm)	a (fm)	σ_R (mb)	Δ
O^{16}	1	60.00	15.00	1.47	0.55	909	1642
	2	53.97	13.15	1.54	0.50	902	1273
	3	50.90	9.76	1.63	0.40	869	920
	4	53.36	10.14	1.62	0.38	863	541
	5	52.66	10.31	1.64	0.40	894	556
	6	52.95	9.97	1.64	0.38	873	530
	7	53.18	9.94	1.63	0.38	867	529
	8	53.15	9.94	1.63	0.38	868	529
Ni^{58}	1	53.00	15.80	1.49	0.57	1587	1748
	2	56.20	18.12	1.56	0.46	1564	1542
	3	53.73	19.20	1.53	0.48	1550	1892
	4	55.56	16.79	1.54	0.46	1540	1724
	5	55.53	16.77	1.54	0.46	1536	1720
	6	55.50	16.78	1.54	0.46	1538	1719
	7	55.51	16.78	1.54	0.46	1537	1719
Pb^{207}	1	50.00	10.00	1.50	0.60	2471	296
Pb^{208}	2	53.83	14.46	1.49	0.52	2325	165
	3	60.64	18.26	1.47	0.55	2336	100

Fixed form factor: $r_0 = 1.50$ fm; $a = 0.65$ fm

Target	Cycle	U (MeV)	W (MeV)	σ_R (mb)	Δ
O^{16}	1	53.00	10.00	933	1777
	2	56.89	12.70	1005	1466
	3	56.85	11.99	994	1431
	4	56.87	11.99	994	1431
Ni^{58}	1	50.00	13.00	1691	3014
	2	52.46	15.16	1718	2303
	3	54.35	14.76	1726	2243
	4	54.13	14.33	1722	2235
Pb^{207}	1	50.00	10.00	2568	410
Pb^{208}	2	52.66	9.52	2584	386
	3	53.80	9.32	2590	381

The fits for Pb^{207} and Pb^{208} were made using all the measured data and the calculated distribution fits them fairly well.

Figs. 1-3 show the angular distributions of elastically scattered deuterons from O^{16}, Ni^{58}, Pb^{207} and Pb^{208}, respectively. Diffraction patterns with characteristic maxima and minima are clearly shown in those corresponding to light and medium nuclei. This structure is smoothed as the target mass number increases and is no longer visible for lead. Within the experimental errors no difference is observed between the Pb^{207} and Pb^{208} elastic angular distributions.

4. Strong Coupling Analysis of (d,d') Inelastic Scattering

The inelastic scattering data were analysed using the strong coupling approximation in which the elastic and first inelastic channels are treated explicitly and the remaining inelastic channels are taken into account through an appropriate absorbing potential. This calculation applies to the $0^+ \rightarrow 2^+$ excitation of even nuclei and makes use of the collective model of the excited state, assuming it to be either rotational or vibrational. These two possibilities give very similar results, and the rotational model is used here. The only additional parameter in this model is the deformation parameter

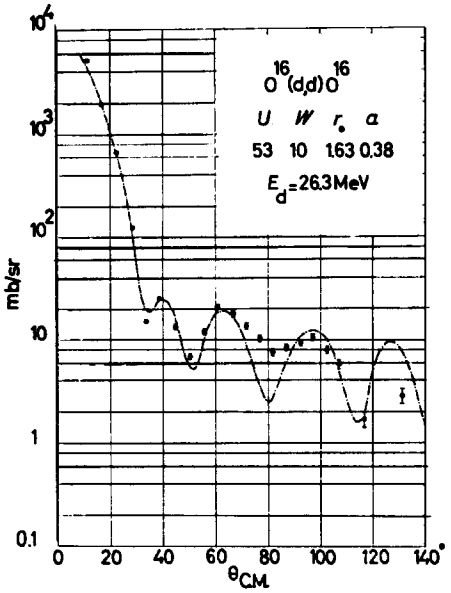

Fig. 1. The elastic scattering of 26.3 MeV deuterons by oxygen-16. The observed cross-sections in the centre-of-mass system are plotted as a function of the centre-of-mass angle. The experimental data are compared with optical model calculations with the parameters given in the inset to the figure.

β of the target nucleus. A full account of the formalism of this model and the mathematical techniques used has been published elsewhere [5]).

The strong coupling model gives the angular distribution of the inelastically scattered ($Q = -1.45$ MeV) deuterons; there is no uncertain normalizing factor though the absolute magnitude may be altered by varying β, if this is not already fixed by other work. The calculation also gives the elastic scattering cross-section. If the same optical parameters are used this is the same in the weak coupling limit ($\beta \rightarrow 0$) as that calculated with the simple optical model, but progressively departs from it as the coupling increases. Ideally the optical model parameters in the strong coupling calculation should be systematically varied to give the best fit to both the elastic and the first inelastic experimental cross-sections. At present this would require a prohibitive

amount of computing time so we simply use the optical parameters already obtained from the analysis of the elastic scattering data. This is justified by the close accord found between the elastic cross-sections given by the strong coupling model and those given by the simple optical model with the same parameters. (See fig. 2).

In the present calculation the deformation parameter β of Ni^{58} was taken to be 0.23 from the analysis of inelastic proton scattering by Buck [5]); the strength of the coupling

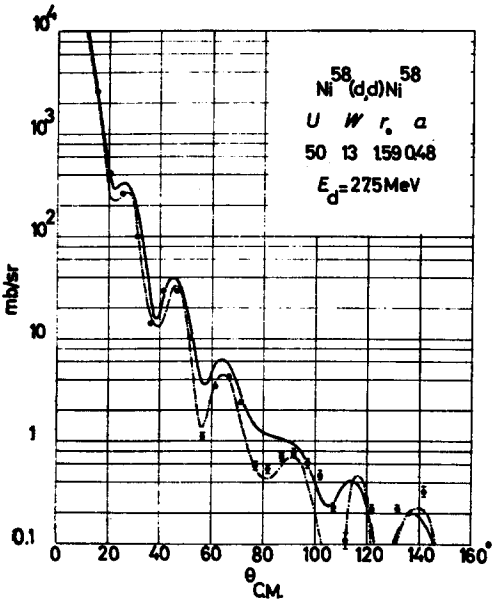

Fig. 2. Same as for fig. 1 for 27.5 MeV deuterons on nickel-58. The full line curve refers to the strong coupling calculation.

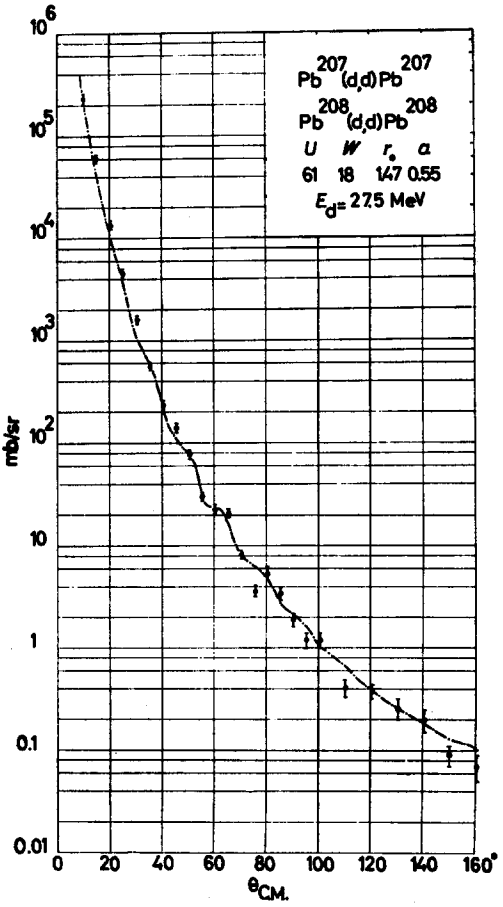

Fig. 3. Same as for fig. 1 for 27.5 MeV deuterons on lead-207 and lead-208.

potential between the elastic and first inelastic channel is then $U_C = \beta RU/(a\sqrt{4\pi})$ = 41.5 MeV. The angular distribution found in this calculation is shown in fig. 4 together with the optical potentials used. There is good overall agreement with the experimental values. Similar fits have been obtained by Satchler [4]) using somewhat different optical parameters and a significantly higher deformation parameter.

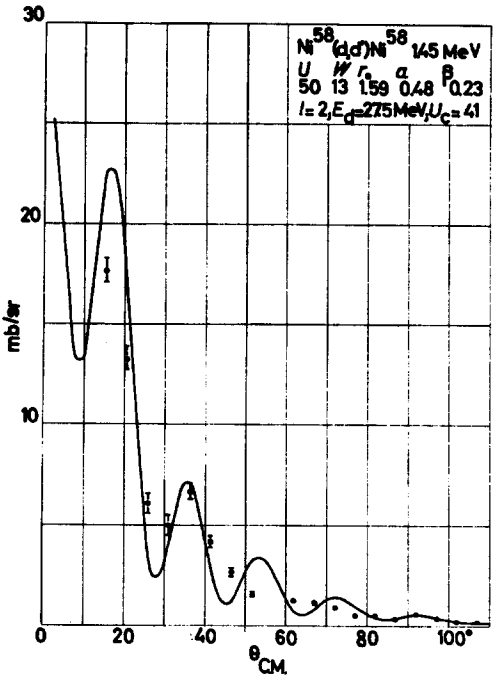

Fig. 4. The inelastic scattering of 27.5 MeV deuterons by nickel-58($Q = -1.45$ MeV). The observed cross-sections for the centre-of-mass system are plotted as function of the centre-of-mass angle. The experimental data are compared with calculations based on the strong coupling approximation. The optical model parameters are shown.

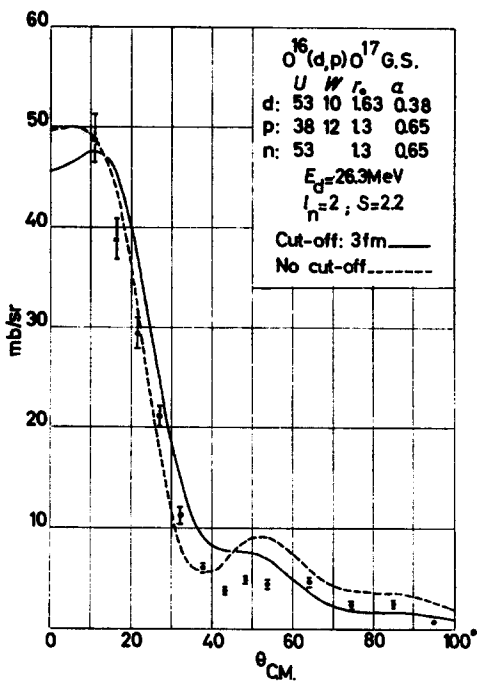

Fig. 5. The stripping of 26.3 MeV deuterons by oxygen-16 to the ground state of oxygen-17. The observed cross-sections for the centre-of-mass system are plotted as functions of the centre-of-mass angle. The experimental data are compared with calculations using the distorted wave Born approximation. The full line curve refers to calculations with a lower cut-off radius of 3 fm, the dashed curve to a calculation without cut-off.

TABLE 3

Optical model parameters used in the (d, p) stripping and (d, d') inelastic scattering calculations

Reaction	Particle	U (MeV)	W (MeV)	r_0 (fm)	a (fm)
O^{16}(d, p)O^{17}(gs)	d	53.1	9.9	1.63	0.38
	p	38	12	1.30	0.65
	n	53		1.30	0.65
O^{16}(d, p)O^{17}(0.872 MeV)	d	53.1	9.9	1.65	0.38
	p	38	12	1.30	0.65
	n	51.1		1.30	0.65
Ni^{58}(d, p)Ni^{59}(gs)	d	49.9	12.7	1.59	0.48
	p	38	12	1.30	0.65
	n	48.1		1.30	0.65
Pb^{207}(d, p)Pb^{208}(gs)	d	60.6	18.3	1.47	0.55
	p	38	12	1.30	0.65
	n	42.4		1.30	0.65
Ni^{58}(d, d')Ni^{58}(1.45 MeV)	d	49.9	12.7	1.59	0.48

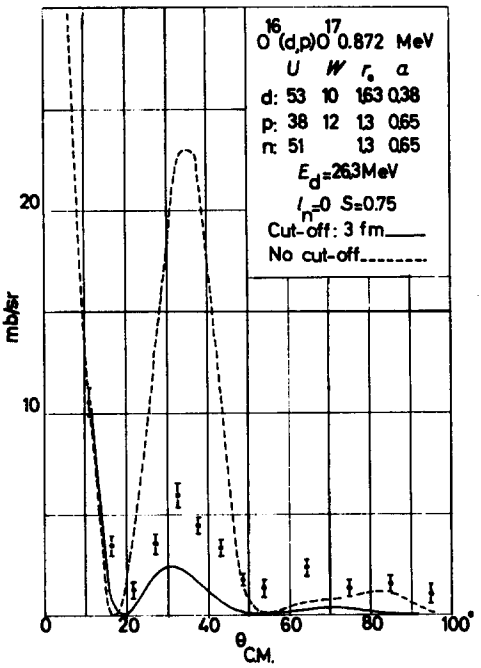

Fig. 6. Same as for fig. 5 but for $O^{16}(d, p)O^{17}$ (0.872 MeV).

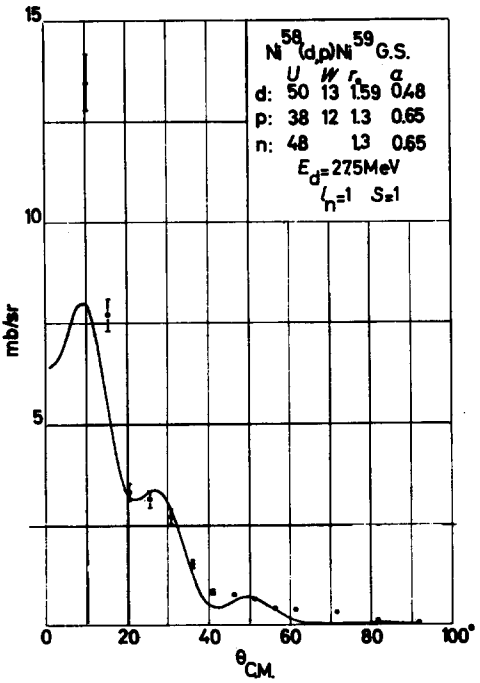

Fig. 7. Same as for fig. 5 but for 27.5 MeV and $Ni^{58}(d, p)Ni^{59}$ (ground state). No cut-off.

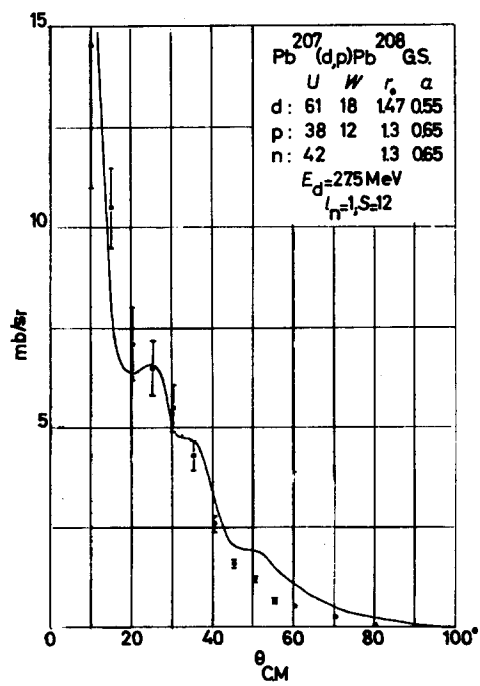

Fig. 8. Same as for fig. 5 for 27.5 MeV deuterons and $Pb^{207}(d, p)Pb^{208}$ (ground state). No cut-off.

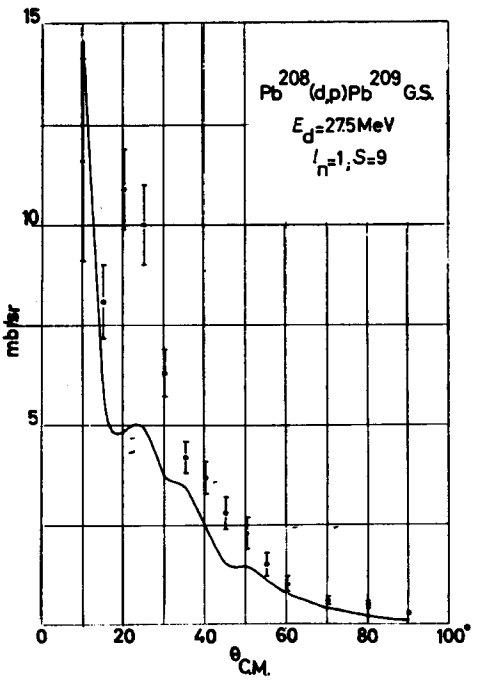

Fig. 9. Same as for fig. 5 for 27.5 MeV deuterons and $Pb^{208}(d, p)Pb^{209}$ (ground state). No cut-off.

5. Distorted Wave Analysis of (d, p) Stripping

Using the deuteron parameters from the optical model elastic scattering analyses of sect. 3 together with proton parameters from similar (p, p) analyses a zero-range distorted wave Born approximation calculation of the (d, p) cross-section was made. The formalism used is described elsewhere [6]) and the calculations were made on an IBM 7090 computer †.

Table 3 shows the parameters used in the present analysis, and figs. 5 and 6 show the angular distribution leading to the ground and first excited states of O^{17} together with the corresponding $l_n = 1$ and $l_n = 0$ theoretical fits.

These cross-sections were computed with and without a lower cut-off in the radial integrals. The cut-off takes into account, in a crude way, some of the effect of the finite range of the neutron-proton interaction and of the non-local character of the nucleon and deuteron-nucleus interaction. The cut-off improves the fit in both cases, particularly in the excited state case. The overall agreement is as good as can be expected for a light element like oxygen.

TABLE 4

Distorted wave Born approximation stripping spectroscopic factors

Reaction	E_d (MeV)	Q (MeV)	l_n	S
O^{16}(d, p)O^{17}(gs)	26.3	1.919	2	2.2[a])
O^{16}(d, p)O^{17}(0.872 MeV)	26.3	1.048	0	0.75[a])
Ni^{58}(d, p)Ni^{59}(gs)	27.5	6.78	1	1
Pb^{207}(d, p)Pb^{208}(gs)	27.5	5.15	1	12
Pb^{208}(d, p)Pb^{209}(gs)	27.5	1.65	1	9

[a]) From cut-off calculation.

Fig. 7 shows the (d, p) angular distribution leading to the Ni^{59} ground state. Here the fit is quite satisfactory for most of the measured points and no normalization was used. The $l_n = 1$ curve is the only one permitted by the selection rules. These data have also been analysed by Satchler [4]).

Figs. 8 and 9 show the corresponding distributions to the Pb^{208} and Pb^{209} ground states. Only the former was fitted because of their similarity; the $l_n = 1$ curve permitted by the selection rules describes the data well if it is appropriately normalized.

These analyses show that the distorted wave analysis gives an adequate fit to the data with a single value of l_n. The same data analysed with the plane-wave theory required a superposition of curves corresponding to two values [2]) of l_n.

The spectroscopic factors S (defined as the ratio of the experimental cross-section divided by the DWBA cross-section) can be extracted from the above calculations; they differ in general from the corresponding factors extracted from plane wave analyses. The present calculations give the values shown in table 4.

† The programme used was written by B. Macefield.

It is a pleasure to thank the technical staff of the synchrocyclotron for their collaboration during the irradiation. Thanks are also due to the head of the Computing Centre at the University of Buenos Aires for his kind permission to use the computer; to Mr. J. Araoz for his help during the computation work; to the Director of the Oxford University Computing Laboratory for the use of the Mercury Computer; to Mr. B. Macefield for arranging for the (d, p) and (d, d') calculations to be made on an IBM 7090 computer at A.W.R.E. Aldermaston, and to the D.S.I.R. for support.

References

1) P. E. Hodgson, The optical model of elastic scattering (Clarendon Press, Oxford, 1963)
2) S. Mayo and J. Testoni, Nuclear Physics **36** (1962) 615
3) B. Buck, R. N. Maddison and P. E. Hodgson, Phil. Mag. **5** (1960) 1181;
R. N. Maddison, Proc. Phys. Soc. **79** (1962) 264
4) G. R. Satchler, private communication
5) B. Buck, Phys. Rev. **130** (1963) 712
B. Buck, A. P. Stamp and P. E. Hodgson, Phil. Mag. **8** (1963) 1805
6) B. Buck and P. E. Hodgson, Phil. Mag. **6** (1961) 1371